

parts of the dielectric function are

$$\epsilon_R(y,z) = 1 + \frac{k_{FT}^2}{2k_F^2} \frac{1}{(z+y)^2} \times \left[ 1 + \frac{1}{2(z+y)} (1-y^2) \ln \left| \frac{1-y}{1+y} \right| - \frac{1}{2(z+y)} (1-z^2) \ln \left| \frac{1+z}{1-z} \right| \right], \quad (\text{A11})$$

$$\epsilon_I(y,z) = \frac{\pi k_{FT}^2}{4k_F^2(z+y)^3} (\lambda^2 - y^2). \quad (\text{A12})$$

A singularity at the Fermi surface will occur if  $f(z)$  is discontinuous at  $z=1$ . From its definition it is easy to see that  $f(z)$  is continuous at  $z=1$ , so that (A9) has no logarithmic singularity at  $\eta=1$ . This cut integral does not contribute any singular behavior to the density of states at the Fermi surface.

## Infrared Lattice Vibrations in $\text{GaAs}_y\text{P}_{1-y}$ Alloys

H. W. VERLEUR\* AND A. S. BARKER, JR.

*Bell Telephone Laboratories, Murray Hill, New Jersey*

(Received 25 April 1966)

The infrared lattice-vibration spectra of mixed crystals of  $\text{GaAs}_y\text{P}_{1-y}$  have been measured by reflection techniques. These crystals exhibit two distinct reststrahlen bands whose strengths and frequencies depend on  $y$  and which show considerable fine structure. A harmonic model has been developed to account for the significant features of these spectra. The main features of the model are (1) the inclusion of a clustering effect or nonrandom distribution of anions on a microscopic scale, (2) the existence of 5 distinct molecular complexes which leads to 2 groups of 4 closely spaced optical phonon modes, and (3) effective ionic charges that have both local and nonlocal parts. The model provides the frequencies and strengths of the optical phonon modes which with suitably chosen damping constants yield a good fit to the reflectivity spectrum over the entire range of solid solutions.

### INTRODUCTION

MIXED crystals (or alloys) of  $\text{GaAs}_y\text{P}_{1-y}$  can be grown over the entire composition range  $y=0$  to 1. These alloys are interesting for several reasons, one being their electronic band structure. GaAs is a direct gap material while GaP has an indirect gap. For the alloy, as  $y$  is increased, the band structure near the gap appears to change continuously, the central  $k=0$  conduction-band minimum falling relative to the other valleys until near  $y=0.6$  the  $k=0$  minimum becomes the lowest valley changing the material from indirect to direct gap and drastically affecting the threshold for laser action and the luminescence properties.

Whereas it is known that the alloys have the same crystal structure as the parent crystals GaP and GaAs (i.e., zinc-blende), the distribution of the constituent ions over the sublattices is not known. One usually assumes that the structure consists of a Ga fcc sublattice and an interpenetrating fcc sublattice over which the As and P ions are randomly distributed. It has been suggested, however,<sup>1</sup> that there may be a tendency for like-negative ions to cluster around positive ions. Such clustering, which tends to make small regions GaAs

rich or GaP rich, should have some characteristic effect on the optical-phonon modes since they depend strongly on nearest-neighbor force constants.

We intend to show in this paper that a detailed analysis of the infrared reflectivity spectrum of  $\text{GaAs}_y\text{P}_{1-y}$  supports the assumption of short-range clustering. A harmonic-oscillator model of the lattice dynamics of the alloy is developed including a short-range order parameter which accounts quantitatively for the significant features of the reflectivity spectrum. The characterization of the lattice modes serves as a useful basis for other work. It will be shown that the composition  $y$  of an unknown sample can be determined from the infrared spectrum. Also, additional infrared effects such as free-carrier susceptibility can be properly evaluated only by first taking account of the pure lattice modes.

The extra degree of freedom provided by the composition  $y$  allows us to probe other features of the lattice dynamics of III-V compounds. Brodsky and Burstein have suggested<sup>2</sup> that the usual assumption of a localized, effective ionic charge on each ion, while probably correct for such ionic crystals as the alkali halides, cannot be properly applied to the III-V compounds. The reason they advance is that the valency electrons of the ions in these compounds have extended wave functions and that, thus, the effective ionic charges of the ions should

\* Work performed in partial fulfillment of requirements for the Ph. D. degree, New York University.

<sup>1</sup> T. L. Larsen, E. E. Loebner, and R. J. Archer, *Bull. Am. Phys. Soc.* **10**, 388 (1965); Y. S. Chen and G. L. Pearson, *ibid.* **10**, 369 (1965).

<sup>2</sup> M. Brodsky and E. Burstein, *Bull. Am. Phys. Soc.* **7**, 214 (1962).

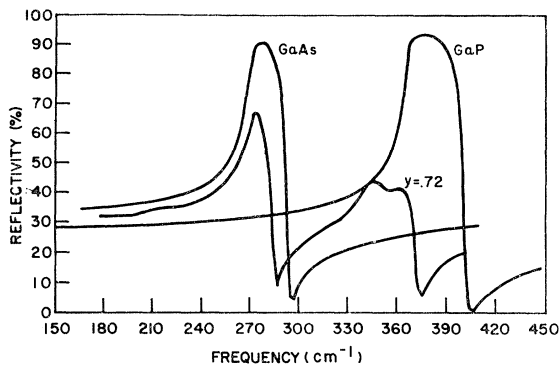


FIG. 1. Reflectivity spectra of GaP, GaAs, and  $\text{GaAs}_y\text{P}_{1-y}$  ( $y=0.72$ ).

have a considerable nonlocal portion. The model developed below supports this assumption and values for the local and nonlocal portions of the effective charge of GaAs and GaP are obtained as "best-fit" parameters to the experimental reflectivity curves. Values for certain force constants are also obtained.

Finally, we believe that the model developed here can, with minor modifications, be used to study the microscopic structure of other mixed crystals.

## EXPERIMENTAL WORK

### Sample Preparation

Samples of  $\text{GaAs}_y\text{P}_{1-y}$  with low carrier concentrations (not exceeding  $10^{16}$  carriers/cm<sup>3</sup>) were obtained covering the entire range of  $y$ . Some of the samples were grown at Bell Laboratories while others were obtained from the Monsanto Company. Whereas the details of the growing techniques of the two suppliers differed somewhat, all crystals were grown from the vapor phase at temperatures around 1100°C.

The Bragg peak from the (111) planes was measured using a double-crystal x-ray spectrometer. The average composition of each crystal, that is the value of  $y$ , was determined from this measurement. The lattice constant was assumed to vary linearly with composition (Vegard's Law) from its value for GaP (5.45 Å) at  $y=0$  to its value for GaAs (5.65 Å) at  $y=1$ . A few samples with high phosphorus concentration showed broad overlapping double peaks whose width almost spanned the Bragg angle between 13°39' (pure GaAs) and 14°10' (pure GaP) suggesting segregation on a macroscopic scale. These samples were not studied further. Typically the mixed crystals had (111) lines whose width at half-maximum height was 5 to 7 min. Pure GaAs samples exhibited a (111) half-width of 1 min and pure GaP about 1.7 min.

The samples were oriented to have their major face parallel to a (111) plane [or in one case parallel to a (211) plane]. They were mechanically polished to a mirror-like finish as well as chemically etched to remove

any surface damage. A careful examination of the crystals whose infrared reflectivity spectra were measured showed no large scale clustering of As or P or other inhomogeneities in average composition. The techniques used to arrive at this conclusion were:

1. Study of the photoluminescence of the crystals to determine excitations due to possible inclusions of pure GaAs. None were found. The excitations that were found corresponded to band-to-band transitions at energies intermediate to those of pure GaAs and GaP and consistent with the known composition of the crystals. The question to be answered here, of course, is, how large a region of pure GaAs must exist before one can observe GaAs band-to-band transitions. Melcher<sup>3</sup> has considered the simple model of a free electron confined to a cubic container of edge  $L$ . He arrived at the conclusion that the volume of this container should be on the order of microns before the difference in adjacent energy levels can be approximated by an energy continuum. This approach probably gives a high estimate in view of the fact that the wavelength of a thermal electron in the conduction band in GaAs (assuming  $m^*=0.1 m_e$ ,  $T=300^\circ\text{K}$ ) is about 200 Å. It appears then that this experiment does not allow us to probe regions extending over only a few atomic diameters. We can conclude that in the GaAs rich samples no regions of pure GaAs extending over one or two microns exist.

2. Study of x-ray fluorescence by means of an electron beam microprobe which allowed us to examine areas as small as three microns in diameter. No variations in composition at this scale were observed and no fluorescence characteristic of pure GaAs or GaP was detected.

### Reflectivity Spectra

The infrared reflectivity spectra for unpolarized light at normal incidence were measured over the frequency range from 100 cm<sup>-1</sup> to 450 cm<sup>-1</sup> by means of a con-

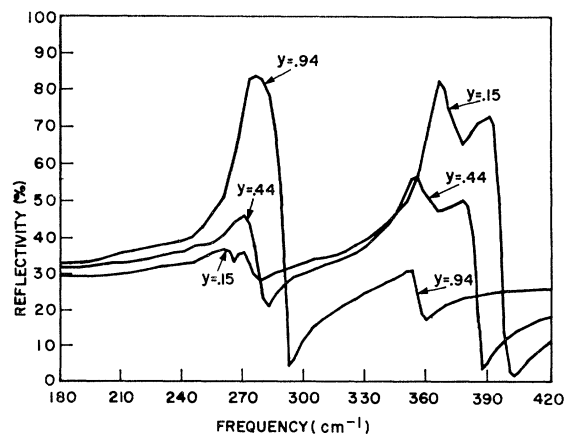


FIG. 2. Reflectivity spectra of three mixed crystals  $\text{GaAs}_y\text{P}_{1-y}$  ( $y=0.15$ ,  $y=0.44$ ,  $y=0.94$ ).

<sup>3</sup> A. G. Melcher, The University of Michigan Engineering Summer Conferences on Semiconductor Theory, 1965 (unpublished).

ventional spectrometer. The general method of taking data has been discussed by others.<sup>4</sup> The experimental conditions allowed a resolution of  $2.5\text{ cm}^{-1}$  for practically all wavelengths investigated. This resolution yields sufficient energy to measure reflectivities with uncertainties of  $\pm 0.5\%$ . Reruns of a sample which included repositioning gave consistent results to within  $\pm 1.0\%$ . The results are shown in Figs. 1 and 2.

### Discussion of Experimental Results

A preliminary report of the reflectivity spectra was given previously.<sup>5</sup> We list here the characteristic features that are to be explained by the model we are about to develop.

1. Two main bands of relatively high reflectivity exist between approximately  $250\text{ cm}^{-1}$  and  $410\text{ cm}^{-1}$  for the entire range of solid solutions, that is, for all values of  $y$ . (See Fig. 2.)

2. The strength of each band depends on  $y$ .

3. The high-frequency band shifts as much as  $30\text{ cm}^{-1}$  to lower frequencies with increasing values of  $y$ , whereas the low frequency band remains stationary to within 2 or  $3\text{ cm}^{-1}$ .

4. Both bands, especially the high frequency one, show considerable fine structure.

We note here that while the reflectivity at the maximum of each reststrahlen band depends on the surface treatment of the specimen (polished or etched), the treatment did not affect the fine structure. In other words, the latter is not due to surface damage, but is an intrinsic property of the crystals. An example of this is shown in Fig. 3 where the peaks of the high-frequency bands are compared for a polished and etched specimen (15% As).

Figure 3 also shows the effect of cooling to  $90^\circ\text{K}$ . The fine structure is not temperature-dependent; however, the entire band shifts to higher frequencies on cooling. A consideration of possible two-phonon sum or difference bands shows that even the most temperature-insensitive combination would predict a reduction in mode strength of at least a factor of 2 on cooling which could easily have been detected.

A Raman-scattering study of one of the mixed crystals ( $y=0.15$ ) using the helium neon  $6328\text{-\AA}$  laser was used to check that the lattice vibration modes are not dependent on surface effects. The Stokes-shifted light was collected from about  $0.25\text{ mm}$  behind the front surface of the crystal. While the signal-to-noise ratio for this experiment was poor because of large Rayleigh scattering, the Raman spectrum showed the two main bands and also the strongest fine structure feature at the same frequencies as they appear in the infrared spectrum of this sample.

<sup>4</sup> W. G. Spitzer and D. A. Kleinman, *Phys. Rev.* **121**, 1324 (1961).

<sup>5</sup> H. W. Verleur and A. S. Barker, Jr., *Bull. Am. Phys. Soc.* **10**, 72 (1966).

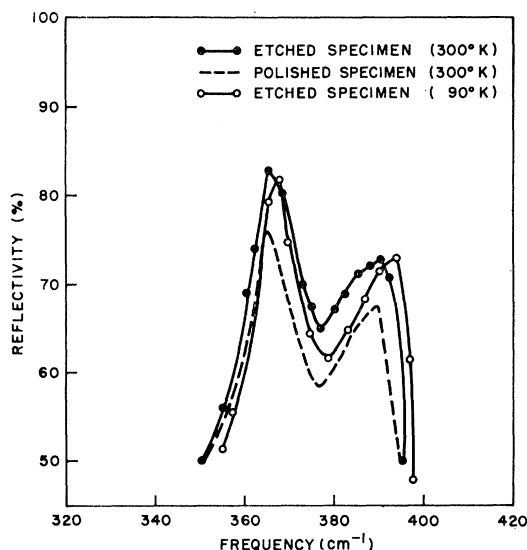


FIG. 3. Comparison of peaks of the high-frequency reflectivity band of  $\text{GaAs}_y\text{P}_{1-y}$  ( $y=0.15$ ) for a polished surface and an etched surface at room temperature and an etched surface at  $90^\circ\text{K}$ .

These results and arguments support in part the conclusions later to be drawn that the fine structure is due to new fundamental vibrational modes of the mixed crystal.

## THEORETICAL MODEL

### Description of a Disordered Alloy

Before describing the model with its basic vibrating units it is appropriate to consider the possible structural configurations of a  $\text{GaAs}_y\text{P}_{1-y}$  mixture. We take the gallium sublattice to be perfect, and so we are really discussing the binary alloy  $\text{As}_y\text{P}_{1-y}$  whose atoms must be distributed over a fcc lattice. Two extremes of behavior are at once apparent. There can be complete segregation where all of the As atoms cluster in one region and all the P in a second region. All anion-anion bonds in the alloy are then As-As or P-P except for the few across the interface separating the regions. For this extreme of behavior the word "alloy" is inappropriate. One other extreme of behavior is the alloy with perfect long-range and short-range order for which  $y=0.25$  or  $y=0.75$  and cubic symmetry is preserved. The available sites divide into two unique groups: the face centers and the cube corners. Putting As ions on all face centers and P ions on all cube corners gives  $\text{GaAs}_{0.75}\text{P}_{0.25}$ . This structure can repeat indefinitely in space. In this structure, half of the anion-anion bonds are As-As and half are As-P. There are no P-P bonds. These are far different proportions than for a segregated mixture of the same composition. Fcc alloys of  $\text{Cu}_{0.75}\text{Au}_{0.25}$  have been studied<sup>6</sup> and found to exhibit the type of order described

<sup>6</sup> J. M. Cowley, *J. Appl. Phys.* **21**, 24 (1950); N. Norman and B. E. Warren, *ibid.* **22**, 483 (1951).

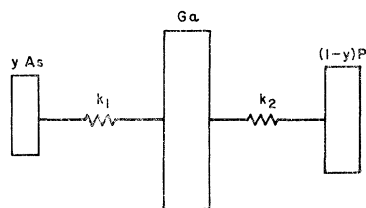


FIG. 4. Simple model of the alloy, assuming independent As-ion and P-ion sublattices which interact only with the Ga-ion sublattice.

here, but with a transition to a more disordered state as the temperature is raised. The partially disordered state covers the considerable intermediate ground between the extremes mentioned. The appropriate parameters used for its description are short-range order probabilities. For example, if we pick a P ion in the  $\text{As}_{0.75}\text{P}_{0.25}$  ordered alloy the probability of finding an As ion as nearest neighbor is 1.0 and as second-nearest neighbor is 0. In the segregated mixture these probabilities are both zero. We can picture an almost random alloy where this probability approaches 0.75 for far-distant neighbors (just the average concentration of As) but retains a value of almost 1.0 for nearest neighbors, indicating that As ions prefer to cluster around a P ion as nearest neighbors but that there is not enough energy gained from this configuration to force the whole crystal into this pattern. Probability considerations such as these will play an important part in the model developed below.

Matossi has discussed the optical vibrations of a 50:50 ordered binary alloy using a linear chain model.<sup>7</sup> With such perfect order one can choose a larger unit cell and proceed as in the case of any perfect lattice. This approach appears to give good accord with the optically active lattice vibrations in some mixed alkali halides where the mixed crystal has one strong infrared mode. Another approach close to this involves the analysis of a virtual crystal which has the same structure as pure GaAs but in which each anion site is occupied by an idealized composite atom which has a mass  $M = \gamma m_a + (1 - \gamma)m_p$  and is bound by a potential which is also the appropriate average. This type of model gives only one optically active mode intermediate to the frequencies of pure GaP and pure GaAs. Neither of these approaches is appropriate here.

Purely random alloys have been treated with a linear chain model by Dean and co-workers.<sup>8</sup> For this model, many characteristic frequencies occur as small spikes in the density of states which can be identified with ordered clusters of 2 atoms, 3 atoms, etc.

The appearance of the reflectivity spectrum of  $\text{GaAs}_y\text{P}_{1-y}$  with its characteristic GaP band and GaAs band suggests that there is a high degree of independence between Ga-As and Ga-P interactions. As a first approximation, we could take a model of the alloy which has a rigid Ga sublattice vibrating independently against both

a rigid As and a rigid P sublattice (see Fig. 4). If we do not consider any interaction between As and P, or between Ga atoms and a combination of As and P atoms, this model would yield two reststrahlen bands. The strength of each band would indeed depend on the amount of As and P present, but the observed dependence of the frequencies on concentration and the fine structure of the bands would not be explained by this simple model.

To obtain these last two features, we must include as a perturbation of the basic model the effect of P on the Ga-As interaction and of As on the Ga-P interaction as well as the interaction between second neighbors (As-As, P-P, Ga-Ga and As-P). To describe the degree of relative independence of the As and P interactions with the Ga sublattice we introduce a parameter  $\beta$ . As applied to our model,  $\beta$  specifies the degree of clustering of like negative ions around a Ga ion. We stress that in the usual language of alloy structure,  $\beta$  would more properly be called a disorder parameter. The two experiments, previously mentioned, do not support any large-scale clustering but would not necessarily contradict the existence of clusters of like negative ions around Ga ions extending to nearest or next-nearest neighbors only. We will, however, even in our model not treat order beyond the nearest neighbors of Ga atoms, since we rapidly approach the situation described by Dean with many more frequencies than are observed in our spectra.

### Basic Units

Each Ga ion has four nearest neighbors which, in the mixed crystal, may be either As or P. Figure 5 shows the

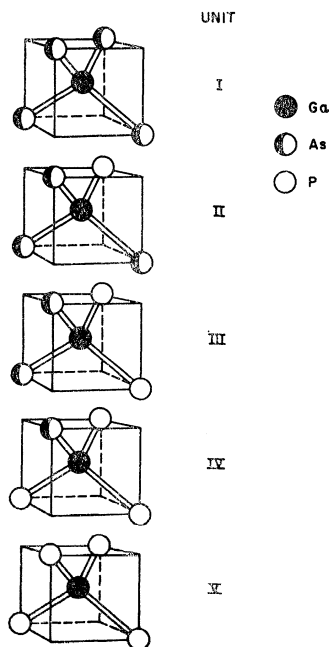


FIG. 5. Basic units of nearest-neighbor ions around a Ga-ion site. Units 2, 3 and 4 must occur in other orientations besides those pictured here to agree with the observed optical isotropy of the mixed crystals.

<sup>7</sup> F. Matossi, *J. Chem. Phys.* **19**, 161 (1951).

<sup>8</sup> P. Dean, *Proc. Roy. Soc. (London)* **A260**, 263 (1961); P. Dean, *Proc. Phys. Soc. (London)* **84**, 727 (1964).

five possible configurations that can exist in the crystal. The As and/or P ions form a tetrahedron with the Ga ion at its center. The entire lattice of the mixed crystal is built up from these five basic units. Since each negative ion is shared by four Ga ions, each unit contains two ions, viz., a Ga ion and one quarter of each of this ion's nearest neighbors. The number of each unit present depends, of course, on the average concentration  $y$ .

Units 1 and 5 have the full symmetry of pure GaAs (or GaP). Units 2, 3, and 4, however, have lower symmetry since the corners of the tetrahedron are occupied by different atoms. Yet, the reflectivity spectrum of the mixed crystal is invariant under rotation about any axis (i.e., the crystal is optically isotropic). This is, of course, due to the fact that throughout the crystal the units 2, 3, and 4 occur randomly in all possible orientations, giving isotropic behavior on a macroscopic scale.

If we now fix our attention on a single bond, say between a Ga and an As ion, we expect that the strength of this bond will in part depend on the other three ions associated with the same Ga ion. In other words, we will represent this bond by a different spring constant depending on the unit this ion pair belongs to. This will take account of the change in overlap forces and distortions of the bonds arising from the introduction of different ions at the corners of the tetrahedron.

Returning to our simple model of Fig. 4, we can no longer consider the As and P ions to form two rigid sublattices, vibrating against a Ga sublattice. For Ga ions we recognize the five different nearest-neighbor environments (or units shown in Fig. 5) and thus introduce five Ga ion coordinates  $w_g(i)$ ,  $i=1$  to 5. Since we deal only with long-wavelength ( $k=0$ ) vibrations, these coordinates each represent the rigid motion of an entire sublattice of a given type of Ga ion. For As or P ions, the nearest neighbors are always four Ga ions, so one would have to go to second neighbors to define different environments. Rather than considering the large number of distinct As ions and P ions defined by these different second-neighbor environments, we instead associate with a given Ga ion one quarter of each of the As and P ions that make up its nearest neighbors, thus forming a basic unit. We then consider the As and P ions of this unit to be bound to the Ga ion of the same unit by a strong, i.e., first-neighbor force. The fact that each As and P ion is shared by three other units is then accounted for by an additional interaction between the As and P ions of the unit under consideration and the Ga ions of the surrounding units. We thus introduce four As-ion and four P-ion sublattice coordinates,  $w_a(i)$ , ( $i=1$  to 4) and  $w_p(i)$ , ( $i=2$  to 5). Although there are five basic units, unit 1 contains no P ions and unit 5 contains no As ions.

Like negative ions belonging to different units can now vibrate out of phase. Hence, second-neighbor interactions will be considered between As-As, P-P, and between Ga-Ga when these ions belong to different units.

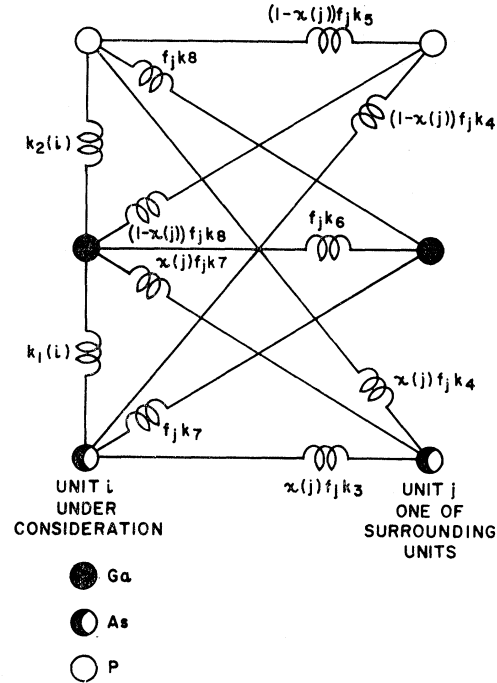


FIG. 6. Schematic diagram of forces on ions in a typical unit type  $i$ . All force constants are indicated. The actual force on an ion is the result of weighting by the probability of occurrence of the bonds shown in the figure and summing over all surrounding ions.

Similarly, we expect second-neighbor interactions between all As and P ions.

In Fig. 6 we have shown all nearest-neighbor and second-neighbor interactions between a unit of type  $i$  and a unit of type  $j$ . The nearest-neighbor force constants are  $k_1(i)$  for As-Ga in unit  $i$  and  $k_2(i)$  for P-Ga in unit  $i$ . The second-neighbor force constants are  $k_3$  for As-As,  $k_4$  for As-P,  $k_5$  for P-P, and  $k_6$  for Ga-Ga interactions. The additional forces between the Ga ions in unit  $i$  and the As ions and P ions in surrounding units  $j$  are represented by  $k_7$  and  $k_8$ , respectively. As mentioned, these forces take account of the sharing of As and P ions by neighboring units.

The actual force on an ion results from weighting the force constants according to the probability of occurrence of all bonds attached to the ion. Figure 6 shows the weighting factors which include the probability coefficients  $f_i$ ;  $f_i$  is the probability of occurrence of basic unit type  $i$ . We also introduce a fractional coefficient  $x(i)$  to take account of the fact that each negative ion is shared by four units. If there are  $N$  ion pairs in the lattice and  $f_i N$  units  $i$ , then there are  $x(i)f_i N$  As ions belonging to units  $i$ , where  $x(i)$  takes on the values  $1, \frac{3}{4}, \frac{1}{2}, \frac{1}{4}$ , and 0 for units 1, 2, 3, 4, and 5, respectively. Consequently, the force constant between the  $i$ th As sublattice and the  $i$ th Ga sublattice in our model normalized to one ion pair is  $x(i)f_i k_1(i)$  and between the  $i$ th P and Ga sublattices it is  $(1-x(i))f_i k_2(i)$ .

We stated earlier that we will consider possible deviations from a random distribution of negative ions up to nearest neighbors of the Ga ions only. This means that we will assume that all negative ions see the same average set of second neighbors, viz.  $12y$  As ions and  $12(1-y)$  P ions. These ions are distributed over the various units such that the fraction of As ions among second neighbors is  $y = \sum_i x(i) f_i$  and the fraction of P ions is  $(1-y) = \sum [1-x(i)] f_i$ . Turning again to our model, this means that the normalized force constant between the  $i$ th As sublattice and the  $j$ th P sublattice is given by  $x(i)(1-x[j]) f_i f_j k_4$ , with similar relations for the other force constants.

### Probability of Occurrence of Basic Units

If one examines the occupancy of a randomly chosen negative ion site in the crystal next to a given Ga ion, the probability that one will find an As ion there is  $y$ , and a P ion,  $1-y$ . This follows from the demonstrated macroscopic homogeneity of the crystal. If the crystal were also microscopically homogeneous, or in other words, if the As and P ions were indeed randomly distributed over their sublattice, then the probability of finding another As ion associated with the same Ga ion would again be  $y$ . It would be independent of the presence of the first-found As ion. We will now assume that this is not necessarily the case. We define the following relations for the probability of finding an As ion next to another As ion ( $P_{aa}$ ) and for the probability of finding a P ion next to another P ion ( $P_{pp}$ ),

$$P_{aa} = y + \beta(1-y), \quad (1)$$

$$P_{pp} = (1-y) + \beta'y, \quad (2)$$

where we have introduced the clustering parameters  $\beta$  and  $\beta'$ . Note that the effect of  $\beta$  is to increase the probability of finding an As ion next to a given As ion. The complementary relations for finding a P ion next to an As ion ( $P_{ap}$ ) and for finding an As ion next to a P ion ( $P_{pa}$ ) are

$$P_{ap} = 1 - P_{aa} = (1-y)(1-\beta), \quad (3)$$

$$P_{pa} = 1 - P_{pp} = y(1-\beta'), \quad (4)$$

and note that it follows from the identity

$$yP_{ap} = (1-y)P_{pa}$$

that  $\beta = \beta'$ . We call  $\beta$  the clustering parameter. After finding these two initial ions of the nearest-neighbor shell around a Ga ion, the probabilities for finding the third As or P ion are

$$P_{aaa} = y + \beta_1(1-y), \quad P_{ppp} = 1 - y + \beta_2 y,$$

$$P_{apa} = y, \quad P_{pap} = (1-y),$$

$$P_{paa} = y, \quad P_{app} = (1-y).$$

Finally, we need the probabilities for the fourth ion to complete the nearest-neighbor shell of anions.

$$P_{aaaa} = y + \beta_3(1-y), \quad P_{pppp} = 1 - y + \beta_4 y,$$

$$P_{aaap} = 1 - P_{aaaa}, \quad P_{pppa} = 1 - P_{pppp},$$

$$P_{apaa} = P_{aa}, \quad P_{papp} = P_{pp},$$

$$P_{apap} = 1 - P_{aa}, \quad P_{papa} = 1 - P_{pp},$$

$$P_{paaa} = P_{aa}, \quad P_{appp} = P_{pp},$$

$$P_{paap} = 1 - P_{aa}, \quad P_{appa} = 1 - P_{pp}.$$

We can express  $\beta_1, \beta_2, \beta_3$ , and  $\beta_4$  in terms of our basic clustering parameter  $\beta$  by using the following identities:

$$\beta_1: \quad yP_{aa}P_{aa} = yP_{ap}P_{apa},$$

$$\beta_2: \quad (1-y)P_{pp}P_{pp} = (1-y)P_{pa}P_{paa},$$

$$\beta_3: \quad yP_{aa}P_{aaa}P_{aaa} = yP_{ap}P_{apa}P_{apa},$$

$$\beta_4: \quad (1-y)P_{pp}P_{ppp}P_{ppp} = (1-y)P_{pa}P_{paa}P_{paa}.$$

Using these probability relations, we can then obtain the following expressions for the fractional distributions,  $f_i$ , of basic units containing 4, 3, 2, 1, or 0 As atoms, respectively:

$$f_1 = y(P_{aa} - y + yP_{aa}^2), \quad (5)$$

$$f_2 = 4y^2P_{aa}(1 - P_{aa}), \quad (6)$$

$$f_3 = 6y^2(1 - P_{aa})^2, \quad (7)$$

$$f_4 = 4(1-y)^2P_{pp}(1 - P_{pp}), \quad (8)$$

$$f_5 = (1-y)(P_{pp} - 1 + y + (1-y)P_{pp}^2). \quad (9)$$

The  $f_i$  must satisfy the following expressions:

$$f_1 + f_2 + f_3 + f_4 + f_5 = 1, \quad (10)$$

$$f_1 + \frac{3}{4}f_2 + \frac{1}{2}f_3 + \frac{1}{4}f_4 = y.$$

Examination of the probability expressions shows that when  $\beta = 0$  the distribution of As and P ions is random depending on the average concentration  $y$  only. When  $\beta = 1$ , the crystal consists of units 1 and 5 only and there is a maximum amount of clustering of like negative ions around the Ga ions.

### Normal Modes and Dielectric Constant

We will consider only forces on the ions arising from pure stretching or compression of the bonds between ions. If we restrict ourselves to vibrations in the direction of an externally applied electric field, the potential energy per ion pair of the system (Fig. 6), is given by<sup>9</sup>

<sup>9</sup> Note that the sublattice force constants  $k_1(i), k_2(i)$  etc. each contain geometrical factors.  $k_1(i)$  for example represents the effect of four bonds extending from the center to the corners of a tetrahedron.  $k_3$  and the other second-neighbor sublattice force constants represent the effects of twelve bonds connecting an ion with its twelve second neighbors.

$$\begin{aligned}
2V = & \sum_{i=1}^5 x(i) f_i k_1(i) (w_\theta(i) - w_a(i))^2 \\
& + \sum_{i=1}^5 (1-x(i)) f_i k_2(i) (w_\theta(i) - w_p(i))^2 + \sum_{i=1}^5 \sum_{j=1}^5 f_i x(j) f_j k_7 (w_\theta(i) - w_a(j))^2 \\
& + \sum_{i=1}^5 \sum_{j=1}^5 f_i (1-x(j)) f_j k_8 (w_\theta(i) - w_p(j))^2 + \sum_{i=1}^5 \sum_{j=1}^5 f_i f_j k_6 (w_\theta(i) - w_\theta(j))^2 \\
& + \sum_{i=1}^5 \sum_{j=1}^5 x(i) x(j) f_i f_j k_3 (w_a(i) - w_a(j))^2 + \sum_{i=1}^5 \sum_{j=1}^5 x(i) (1-x(j)) f_i f_j k_4 (w_a(i) - w_p(j))^2 \\
& + \sum_{i=1}^5 \sum_{j=1}^5 (1-x(i)) (1-x(j)) f_i f_j k_5 (w_p(i) - w_p(j))^2 - 2 \sum_{i=1}^5 f_i (x(i) e_a + [1-x(i)] e_p) w_\theta(i) E_{\text{eff}} \\
& + 2 \sum_{i=1}^5 f_i x(i) e_a w_a(i) E_{\text{eff}} + 2 \sum_{i=1}^5 f_i (1-x(i)) e_p w_p(i) E_{\text{eff}} - \alpha E_{\text{eff}}^2, \quad (11)
\end{aligned}$$

where  $w_\theta(i)$ ,  $w_a(i)$ , and  $w_p(i)$  are the displacements from equilibrium of the Ga, As, and P ions, respectively. The  $e_a$  and  $e_p$  are the total effective ionic charges for As and P. It is assumed that the effective charge on the Ga ion is the linear combination of  $e_a$  and  $e_p$  that makes the unit neutral.

Upon introducing the ionic masses  $m_\theta$ ,  $m_a$ , and  $m_p$ , the kinetic energy of vibration is

$$2T = \sum_i f_i m_\theta \dot{w}_\theta(i)^2 + \sum_i x(i) f_i m_a \dot{w}_a(i)^2 + \sum_i (1-x(i)) f_i m_p \dot{w}_p(i)^2, \quad (12)$$

and the equations of motion can now be written down from Eqs. (11) and (12) by using

$$f_i m_\theta \ddot{w}_\theta(i) = - \frac{\partial V}{\partial w_\theta(i)}$$

and similar relations for the As and P equations. We obtain

$$\begin{aligned}
f_i m_\theta \ddot{w}_\theta(i) = & -x(i) f_i k_1(i) (w_\theta(i) - w_a(i)) - (1-x(i)) f_i k_2(i) (w_\theta(i) - w_p(i)) \\
& - f_i k_7 \sum_{j=1}^5 x(j) f_j (w_\theta(i) - w_a(j)) - f_i k_8 \sum_{j=1}^5 (1-x(j)) f_j (w_\theta(i) - w_p(j)) \\
& - f_i k_6 \sum_{j=1}^5 f_j (w_\theta(i) - w_\theta(j)) + f_i [x(i) e_a + (1-x(i)) e_p] E_{\text{eff}}, \quad (13)
\end{aligned}$$

$$\begin{aligned}
x(i) f_i m_a \ddot{w}_a(i) = & x(i) f_i k_1(i) (w_\theta(i) - w_a(i)) \\
& + x(i) f_i k_7 \sum_{j=1}^5 f_j (w_\theta(j) - w_a(i)) - x(i) f_i k_3 \sum_{j=1}^5 x(j) f_j (w_a(i) - w_a(j)) \\
& - x(i) f_i k_4 \sum_{j=1}^5 (1-x(j)) f_j (w_a(i) - w_p(j)) - x(i) f_i e_a E_{\text{eff}}, \quad (14)
\end{aligned}$$

$$\begin{aligned}
(1-x(i)) f_i m_p \ddot{w}_p(i) = & (1-x(i)) f_i k_2(i) (w_\theta(i) - w_p(i)) \\
& + (1-x(i)) f_i k_8 \sum_{j=1}^5 f_j (w_\theta(j) - w_p(i)) - (1-x(i)) f_i k_4 \sum_{j=1}^5 x(j) f_j (w_p(i) - w_a(j)) \\
& - (1-x(i)) f_i k_5 \sum_{j=1}^5 (1-x(j)) f_j (w_p(i) - w_p(j)) - (1-x(i)) f_i e_p E_{\text{eff}}. \quad (15)
\end{aligned}$$

There are five equations ( $i=1, 2, 3, 4, 5$ ) of type (13) since there is a Ga ion in each unit. Equations (14) and (15) each stand for four equations since units 1 and 5 contain no P or As ions, respectively. We expect these 13 equations to yield 12 optic modes and 1 acoustic mode when the dynamical matrix is diagonalized. This procedure is carried out in the Appendix. Before proceeding to the solution however, we must eliminate the local field  $E_{\text{eff}}$  which appears as a driving force.

In the usual treatment for a diatomic cubic crystal<sup>10</sup> the effective or local electric field is given by

$$E_{\text{eff}} = E + (4\pi/3)P, \quad (16)$$

where  $E$  is the macroscopic electric field and  $P$  is the macroscopic polarization. For our model the dielectric polarization is obtained from Eqs. (11) and (12) by differentiating the energy density with respect to  $E_{\text{eff}}$  and multiplying by  $N$

$$P = N \sum_{j=1}^5 f_j [(x(j)e_a + [1-x(j)]e_p)w_a(j) - x(j)e_a w_a(j) - (1-x(j))e_p w_p(j)] + N\alpha E_{\text{eff}}. \quad (17)$$

The first term in this expression is the polarization due to the atomic displacements and the second term represents the contribution from the electronic polarization of the atoms.  $N$  is the number of units or ion pairs per unit volume and depends on  $y$  since  $N=4/a_0^3$ . For this structure  $a_0$  the lattice constant varies linearly with  $y$ .  $\alpha$  is the electronic polarization per basic unit.

Since upon averaging the basic units, to conform to the isotropy requirements, we take a virtual ion,  $(x(i)\text{As} + [1-x(i)]\text{P})$  to exist at each negative ion site in the lattice, Eq. (16) for the local field might also be used in the present case if the ions could be approximated by point charges. As mentioned earlier, however, for the III-V compounds the valence electrons have extended wave functions. This fact suggests that the effective field is closer to  $E$  than to  $E + 4\pi P/3$ . Following Burstein and Brodsky's suggestion we divide the effective ionic charge into a local and nonlocal portion<sup>2,11</sup>:

$$\begin{aligned} e_a &= e_{a_l} + e_{a_{nl}}, \\ e_p &= e_{p_l} + e_{p_{nl}}. \end{aligned} \quad (18)$$

The effective field acting on the nonlocal charge is then just  $E$ , whereas

$$E_{\text{eff}} = E + (4\pi/3)P_{\text{loc}} \quad (19)$$

is the effective field experienced by the local charge.  $P_{\text{loc}}$  is the atomic displacement polarization arising

from the local effective charge:

$$P_{\text{loc}} = N \sum_{j=1}^5 f_j [(x(j)e_{a_l} + [1-x(j)]e_{p_l})w_a(j) - x(j)e_{a_l}w_a(j) - (1-x(j))e_{p_l}w_p(j)]. \quad (20)$$

We can now eliminate  $E_{\text{eff}}$  in the equation of motion to obtain the mode amplitudes in terms of the driving force  $E$ . Elimination of the mode amplitudes between the equation of motion and the polarization equation gives  $P$  in terms of  $E$ . The dielectric constant is defined in the usual way

$$\epsilon(\omega, y, \beta) = 1 + 4\pi P/E, \quad (21)$$

where we have explicitly shown the frequency dependence, the concentration and clustering dependence. In the Appendix we obtain  $\epsilon(\omega, y, \beta)$  in terms of classical oscillators, or modes, arising from the diagonalization of the dynamical matrix. The 13 modes arising from the 13 degrees of freedom break up into one acoustic mode, four optic modes of almost zero strength and rather low frequencies ( $\sim 100 \text{ cm}^{-1}$ ) and eight infrared active modes in the frequency range 240 to 380  $\text{cm}^{-1}$ . The four inactive modes consist predominantly of entire units vibrating against each other with little relative motion of positive and negative ions. Modes of this type have been discussed by Matossi in his work on the 50:50 linear chain of mixed alkali halides.<sup>7</sup> We add damping to the infrared active modes so that the mode parameters are  $4\pi\rho_j$ ,  $\omega_j$ ,  $\Gamma_j$ , the strengths, frequencies, and damping factors with  $j=1, 2, \dots, 8$ . The high-frequency dielectric constant was computed from the known constants of GaP and GaAs by the assumed relation,

$$\epsilon_{\infty}(\text{GaAs}_y\text{P}_{1-y}) = y\epsilon_{\infty}(\text{GaAs}) + (1-y)\epsilon_{\infty}(\text{GaP}). \quad (22)$$

The theoretical reflectivity is calculated from

$$R(\omega, y, \beta) = \left| \frac{\epsilon^{1/2} - 1}{\epsilon^{1/2} + 1} \right|^2 \quad (23)$$

and compared with the experimental data. The unknown constants involved in the computation of  $R(\omega, y, \beta)$  are the eight nearest-neighbor force constants, plus the two corrections  $k_7$ , and  $k_8$ , the four next-nearest neighbor force constants, the local effective charges of GaP and GaAs, and the clustering parameter  $\beta$ . Finally, the  $\Gamma_j$  are chosen to obtain a best fit to the reflectivity curves. The fitting consisted of successive trials varying the unknown constants, to obtain a best fit to the experimental reflectivity. The general technique of reflectivity fitting, with adjustable mode parameters, has been discussed by others.<sup>12</sup> The method used here of

<sup>10</sup> M. Born and K. Huang, *Dynamical Theory of Crystal Lattices* (Clarendon Press, Oxford, England, 1954), Chap. 2, Sec. 9.

<sup>11</sup> E. Burstein, in *Phonons and Phonon Interactions*, edited by Thor A. Bak (W. A. Benjamin, Inc., New York, 1964), p. 276.

<sup>12</sup> W. G. Spitzer, D. A. Kleinman, and D. Walsh, *Phys. Rev.* **113**, 127 (1959); W. Spitzer, D. Kleinman, and C. J. Frosch, *ibid.* **113**, 133 (1959).

TABLE I. Physical constants used in the calculations of the model.

	Constant	Value
Mass	$m_a$	$11.6 \times 10^{-23}$ g
	$m_a$	$12.4 \times 10^{-23}$ g
	$m_p$	$5.1 \times 10^{-23}$ g
Charge	$e_a$	$10.75 \times 10^{-10}$ esu
	$e_p$	$9.7 \times 10^{-10}$ esu
Dielectric constant	$\epsilon_\infty(\text{GaAs})$	10.9
	$\epsilon_\infty(\text{GaP})$	8.457
Lattice constant	$a_0(\text{GaAs})$	5.65 Å
	$a_0(\text{GaP})$	5.45 Å
Ion pair density	$N_{\text{GaAs}}$	$2.22 \times 10^{22}$ cm $^{-3}$
	$N_{\text{GaP}}$	$2.47 \times 10^{22}$ cm $^{-3}$

adjusting force constants and charges requires some additional comments which are given below.

### FORCE CONSTANTS AND CHARGES USED IN FITS

The large number of unknown constants, as well as the requirement that a good fit to the experimental data be obtained for any value of  $y$ , makes this trial and error procedure a lengthy one. We present, now, some of the considerations that were helpful in establishing orders of magnitude of these constants before an actual fit was attempted. This involved some calculations using data other than reflectivity measurements to compute some of the fitting constants independently. We have listed the known physical constants used in these calculations, in Table I.

There are three sets of force constants, namely, the eight first-neighbor force constants  $k_1(i)$  and  $k_2(i)$ , the two corrections to these force constants which take account of the atom sharing of neighboring units,  $k_7$  and  $k_8$ , and the four second-neighbor force constants,

TABLE II. Classical oscillator parameters determined by curve fitting.

Nearest-Neighbor Force Constants (g/sec $^2$ )		
Symbol	Ga-As force constant	Ga-P force constant
$k_1(1)$	$12.82 \times 10^4$	
$k_1(2)$	$13.52 \times 10^4$	
$k_1(3)$	$14.82 \times 10^4$	
$k_1(4)$	$18.82 \times 10^4$	
$k_2(2)$		$15.5 \times 10^4$
$k_2(3)$		$14.5 \times 10^4$
$k_2(4)$		$13.7 \times 10^4$
$k_2(5)$		$11.5 \times 10^4$
$k_7$	$5.0 \times 10^4$	
$k_8$		$5.5 \times 10^4$
Next-nearest-neighbor force constants (g/sec $^2$ )		
Symbol	Between atoms	Force constant
$k_3$	As-As	$-2.0 \times 10^4$
$k_4$	As-P	$-1.0 \times 10^4$
$k_5$	P-P	$2.75 \times 10^4$
$k_6$	Ga-Ga	$2.0 \times 10^4$
Local effective ionic charges (esu)		
$e_{a1}$		$5.0 \times 10^{-10}$
$e_{p1}$		$1.0 \times 10^{-10}$

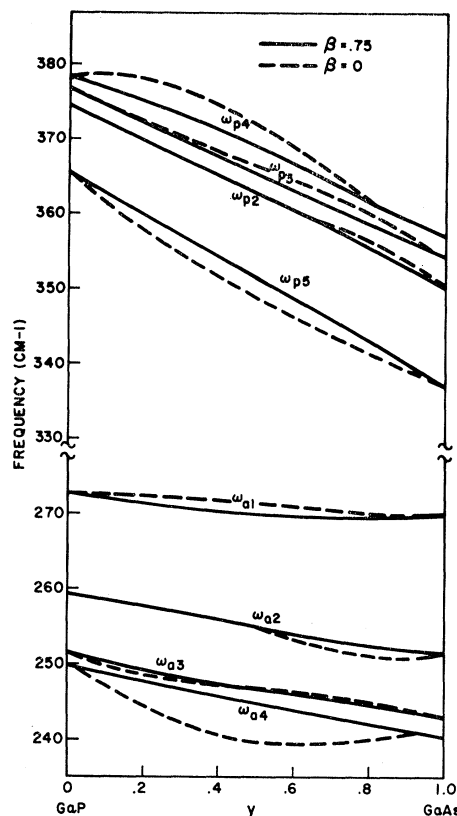


FIG. 7. Mode frequencies versus composition ( $y$ ) computed from the model for  $\beta=0$  and  $\beta=0.75$ . Frequencies are labeled to indicate the principle vibrating ions, i.e.,  $\omega_{a1}$  is frequency of mode consisting mainly of As vibrating against Ga in unit 1, etc.

$k_3, k_4, k_5$ , and  $k_6$ . We expect the three sets to be related as follows:

$$k_1(i), k_2(i) > k_7, k_8 > k_3, k_4, k_5, k_6.$$

The shell-model calculations by Dolling and Waugh<sup>13</sup> for GaAs suggest that second-neighbor force constants are at most  $\frac{1}{10}$  of the first-neighbor force constants and can be positive or negative. For these magnitudes, the requirement of a stable lattice (i.e., no imaginary eigenfrequencies) implies that the first two sets of force constants must be positive.

From available data on the pure materials (GaAs and GaP) we can now establish starting values for some of the fitting constants. The transverse optic (TO) frequency of GaAs for our model is given by

$$\left[ \left( k_1(1) + k_7 - \frac{4\pi}{3} N e_{a1}^2 \right) / \left( \frac{m_g m_a}{m_g + m_a} \right) \right]^{1/2} \quad (24)$$

We can obtain the short-range force constants in this expression from their relation to the empirically known

<sup>13</sup> G. Dolling and J. L. T. Waugh, *Lattice Dynamics* (Pergamon Press, Inc., Oxford, England, 1965), paper A2.

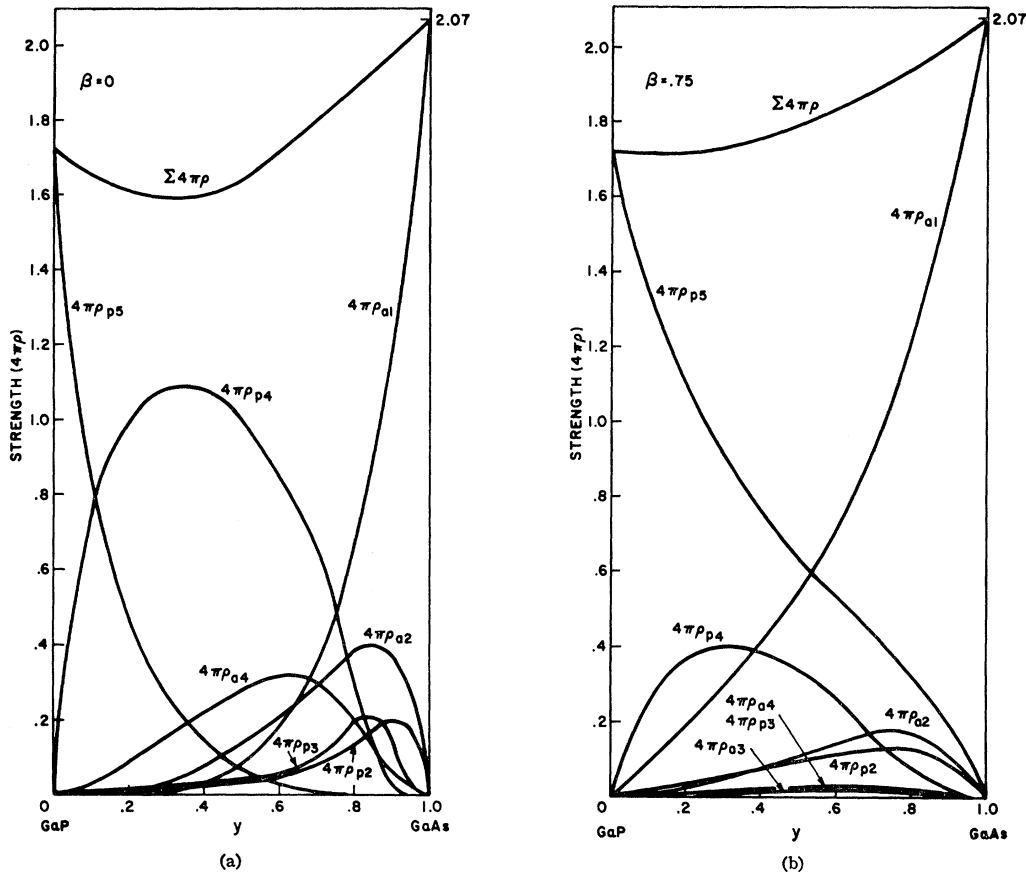


FIG. 8. (a) Mode strengths versus composition ( $y$ ) computed from the model for  $\beta=0$ . Labeling corresponds to Fig. 7; (b) mode strengths versus composition ( $y$ ) computed from the model for  $\beta=0.75$ . Labeling corresponds to Fig. 7.

compressibility<sup>10</sup>:

$$k_1(1) + k_7 = 4\alpha_0 / B_{\text{GaAs}}, \quad (25)$$

where  $\alpha_0$  is the lattice constant, listed in Table I, and the compressibility  $B_{\text{GaAs}} = 1.32 \times 10^{-12} \text{ cm}^2/\text{dyn}$ .<sup>14</sup>

This gives for  $k_1(1) + k_7$  an approximate value of  $17.12 \times 10^4 \text{ g/sec}^2$ . Using the known TO frequency for GaAs ( $270 \text{ cm}^{-1}$ ), we can now solve for  $e_{a1}$  from Eq. (24) and find

$$e_{a1} = 4.1 \times 10^{-10} \text{ esu}.$$

Since the derivation of Eq. (25) completely ignores van der Waal's forces as well as overlap forces between

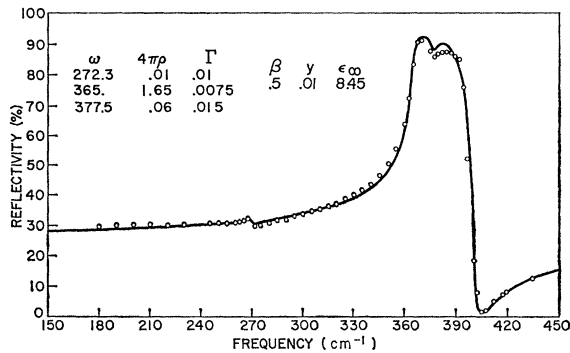


FIG. 9. Theoretical fit (solid line) to experimental reflectivity data for  $y=0.01$ . The oscillator parameters and  $\beta$  value are shown in the figure.

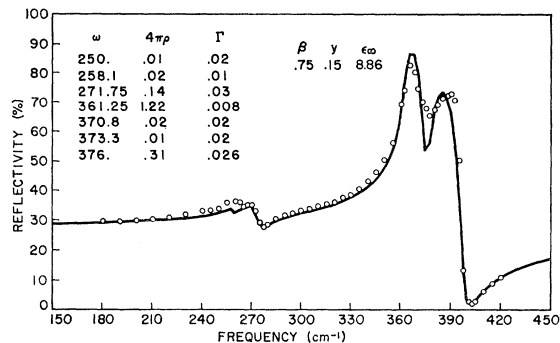


FIG. 10. Theoretical fit (solid line) to experimental reflectivity data for  $y=0.15$ . The oscillator parameters and  $\beta$  value are shown in the figure.

<sup>14</sup> G. L. Pearson and F. L. Vogel, *Progress in Semiconductors* (John Wiley & Sons, Inc., New York, 1962), Vol. 6, p. 9.

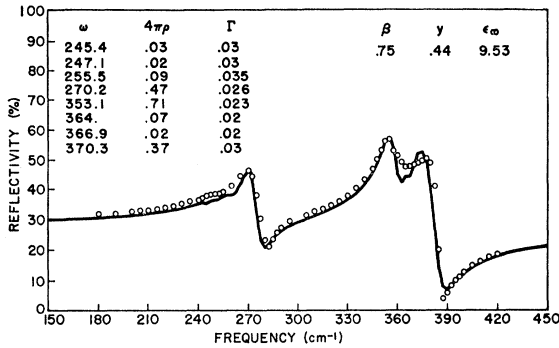


FIG. 11. Theoretical fit (solid line) to experimental reflectivity data for  $y=0.44$ . The oscillator parameters and  $\beta$  value are shown in the figure.

second neighbors and deviations from the ideal ionic structure, a discrepancy can be expected. The values, finally chosen to give the best fit to the reflectivity curves for all values of  $y$ , are  $k_1(1)+k_7=17.82 \times 10^4$  g/sec<sup>2</sup> and  $e_{a_i}=5.0 \times 10^{-10}$  esu (see Table II). In this case, the starting and final values are indeed quite close.

In the case of GaP, the compressibility has recently been measured by Weil.<sup>15</sup> He obtains  $B_{\text{GaP}}=1.12 \times 10^{-12}$  cm<sup>2</sup>/dyn. Using the value for  $\alpha_0$  of GaP from Table I, we obtain

$$k_2(5)+k_8=19.5 \times 10^4 \text{ g/sec}^2.$$

The TO frequency of GaP for our model is given by

$$\left[ \left( k_2(5)+k_8 - \frac{4\pi}{3} N e_{p_i}^2 \right) / \left( \frac{m_0 m_p}{m_0 + m_p} \right) \right]^{1/2} \quad (26)$$

which is equal to 365 cm<sup>-1</sup>. When we solve this for  $e_{p_i}$ , we obtain  $e_{p_i}=5.2 \times 10^{-10}$  esu.

The values finally chosen to give a best fit to the reflectivity curves are,  $k_2(5)+k_8=17.0 \times 10^4$  g/sec<sup>2</sup> and  $e_{p_i}=1.0 \times 10^{-10}$  esu. The difference between starting and final values here is considerably greater than in the case

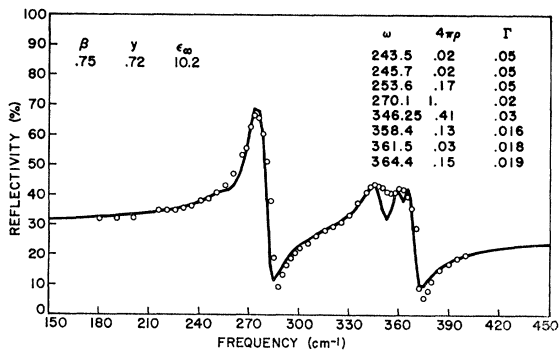


FIG. 12. Theoretical fit (solid line) to experimental reflectivity data for  $y=0.72$ . The oscillator parameters and  $\beta$  value are shown in the figure.

<sup>15</sup> R. Weil (private communication).

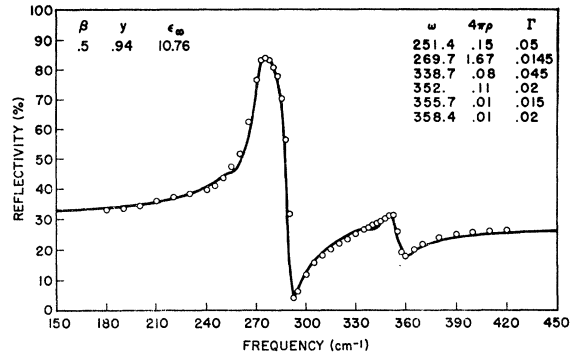


FIG. 13. Theoretical fit (solid line) to experimental reflectivity data for  $y=0.94$ . The oscillator parameters and  $\beta$  value are shown in the figure.

of GaAs. The small value we find for  $e_{p_i}$  is consistent with the unusually small ionicity of GaP observed by others.<sup>15</sup>

The other nearest-neighbor force constants were selected to give the fine structure observed in the reststrahlen bands which is due to the presence of more than two modes. The high-frequency band (P band) consists of a relatively strong mode and weaker modes of higher frequencies. The low-frequency band (As band) has the weaker modes at lower frequencies; they are clearly discernible only at the lower values of  $y$ . (See Figs. 1 and 2.)

In our first attempts to obtain the mode frequencies we neglected the second-neighbor force constants, and chose  $\beta=0$ .  $k_7$  and  $e_{a_i}$  determine the frequency shift with concentration of the main As mode. Values for these constants can be determined by fits to the main As mode frequency at the extremes of the concentration range. Similarly,  $k_8$  and  $e_{p_i}$  can be established by fitting the main P mode frequency.

To obtain the observed frequency shifts of the weaker modes, it was necessary to choose nonzero values for the second-neighbor force constants.

It is found that the choice of force constants has a small effect on the relative strength of each mode. The mode strengths, are mainly controlled by the clustering parameter  $\beta$ . In Figs. 7 and 8 we have plotted the strengths and frequencies of the eight modes as functions of  $y$  for  $\beta=0$  (the random case) and  $\beta=0.75$ , but for the same choice of force constants and local charges. Whereas there is some effect on the frequencies (Fig. 7), the main effect of  $\beta$  is to reduce the number of mixed basic units in the crystal and thus to suppress the strengths of the modes arising from the presence of these units. The final reflectivity fits included adjustments of  $\beta$  as well as small changes in all the force constants to give good fits for all concentrations. All force constants and changes are listed in Table II.

In Figs. 9 to 13 we compare the theoretical fit with the experimentally obtained reflectivity spectra for five mixed crystals. The strengths, frequencies and line-

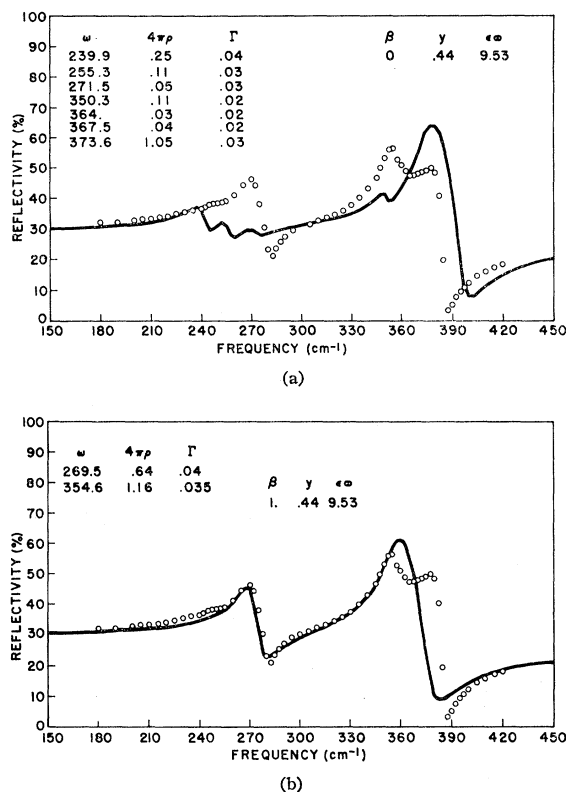


FIG. 14. (a) Theoretical fit (solid line) to experimental reflectivity data for  $y=0.44$ . The force constants and charges are the same as in Fig. 11, but  $\beta=0$ , which results in a complete redistribution of strength between the modes; (b) theoretical fit (solid line) to experimental reflectivity data for  $y=0.44$ . The force constants and charges are the same as in Fig. 11, but  $\beta=1$ , which yields only two infrared active modes.

widths of the modes as well as  $\epsilon_{\infty}$  for each case are listed in the figures.

In Figs. 14(a) and 14(b) we present reflectivity curves for  $\beta=0$ , and  $\beta=1$ , respectively, when  $y=0.44$ . Comparison with Fig. 11 shows the importance of varying only  $\beta$ , the clustering parameter. All other constants were taken the same in these three cases. Even though we could improve the fit in the  $\beta=0$  case somewhat by a variation of the other constants, a good fit could be obtained only for  $\beta=0.75$  as used in Fig. 11.

### LOCAL MODES

It is possible to make some contact with the theory of local impurity modes for the cases of low concentrations of As in GaP and low concentrations of P in GaAs. Tractable theories for impurity modes are available only for low concentrations and for impurities which are mass defects.<sup>16</sup> This last condition is violated to some extent in the GaAs-P case where we find that the nearest neighbor Ga-As bond has about 5% more strength

than the Ga-P bond. We discuss first the case of P in GaAs. Since we are replacing As by a lighter ion we have the possibility of two local modes; one rising out of the acoustic band and one out of the optical band. Since GaAs apparently has no gap,<sup>13</sup> the only possibility for a sharp local mode is the optical-band mode. To find the frequency for this mode, one needs the eigenvectors and eigenvalues for the unperturbed (GaAs) lattice. To get a crude estimate we note that Ga and As have about the same mass so that, as in the case of silicon and germanium, we do not need the eigenvectors. The eigenvalue information is contained in the density of states. A shell model has been fit to neutron data for pure GaAs and a density of states is available.<sup>13</sup> A study of this density of states shows that it is very similar to that of silicon<sup>16</sup> if all silicon frequencies are multiplied by 0.57. (Straight scaling according to the mass would suggest multiplication by 0.62.) Dawber and Elliott have given the local-mode frequencies in silicon as a function of the mass defect parameter  $\epsilon$ .<sup>16</sup> In our case,  $\epsilon = +0.57$ . In silicon, this value gives a local mode at  $628 \text{ cm}^{-1}$ . In GaAs then, by simple scaling we expect a local mode at  $628 \times 0.57 = 357 \text{ cm}^{-1}$ . If we examine our reflectivity fits for the lowest concentration of P in GaAs which was studied ( $y=0.94$ ) we find that the strongest of the impurity modes is at  $352 \text{ cm}^{-1}$ . Furthermore, our calculation of the eigenvector of this mode shows that its amplitude is mostly composed of P vibrating against Ga in unit type 2 (a unit with three As ions and one P ion surrounding a Ga-ion). This type of vibration corresponds most closely to our notion of a localized vibration with a single P ion in an As environment. The theory of Dawber and Elliott can also be used to predict very roughly the strength of the local mode. Using their displacement matrix element, for silicon at  $\epsilon=0.57$ , we find that our case of 6% P in GaAs predicts that the  $352 \text{ cm}^{-1}$  mode should have an oscillator strength of  $4\pi\rho \approx 0.1$ . This strength can be expected to be low, however, since it is derived from a theory of vibrations in a homopolar lattice. The impurity mode in an ionic lattice will move the surrounding ions somewhat giving an effectively larger dipole moment. Calculations of the impurity vibration in GaAs using the Dolling and Waugh density of states have recently been carried out by Taylor. This work predicts a local mode of strength  $4\pi\rho=0.15$  at  $347 \text{ cm}^{-1}$ . Our fits to the 6% P in GaAs sample give a mode of strength of 0.11 at  $352 \text{ cm}^{-1}$ . This is reasonable agreement though we must recall that because of the clustering effect, there is a second impurity mode at  $339 \text{ cm}^{-1}$  with strength 0.08. If we had set  $\beta=0$  in our calculations these two impurity modes would merge and have a total strength of 0.2 compared with the 0.15 given by the local-mode calculation.

We now turn to the case of As impurities in GaP. Experimentally we observe an impurity mode at  $272 \text{ cm}^{-1}$  with a strength of 0.01 when the concentration is about 1% (Fig. 9). Neither a density of states nor

<sup>16</sup> P. G. Dawber and R. J. Elliott, Proc. Roy. Soc. (London) **A273**, 222 (1963); also Proc. Phys. Soc. (London) **81**, 453 (1963).

neutron-diffraction dispersion curves are available for GaP so any estimates must be very qualitative. Since we are replacing a light ion with a heavy one, we have the possibility of a local mode dropping from the optic band into the gap (if it exists) between the optic- and acoustic-mode frequencies. An examination of second-order infrared absorption<sup>17</sup> and Raman scattering data<sup>18</sup> shows that there may be a gap in the phonon spectrum of GaP extending from approximately 200 to 350  $\text{cm}^{-1}$ . Jaswal has considered the corresponding local-mode problem in NaI.<sup>19</sup> NaI has a gap in the phonon spectrum; unfortunately while it serves as an example of a diatomic lattice with unequal masses, the masses are much more disparate than in GaP. We would also expect the phonon dispersion curves to be somewhat different for the two materials. Jaswal's calculation does show that for a mass defect parameter of  $-1.41$  (corresponding to As replacing P) a local mode would appear in his NaI model about centered in the gap. For our estimate of the possible gap in GaP, this result suggests a local mode at about 275  $\text{cm}^{-1}$  if simple frequency scaling is valid. The experimentally observed impurity mode in  $\text{GaAs}_{0.01}\text{P}_{0.99}$  occurs at 272  $\text{cm}^{-1}$ . It appears then that the weak modes in the low concentration alloys, at both ends of the concentration range, are consistent with simple local-mode theory. The purpose, of course, of the model developed in this paper is to take account of interactions and finite concentration effects which are not included in the usual local-mode theories.

### CONCLUSIONS

We have established a model that can account for the significant features of the reflectivity spectra of  $\text{GaAs}_y\text{P}_{1-y}$  for all values of  $y$ . An essential feature of the model is the tendency towards clustering of like ions on the anion sites. For example, with  $\beta=0.75$ , the  $f_i$  have the following value for the 50:50 alloy ( $y=0.5$ )

$$\begin{aligned} f_1 &= 0.38, \\ f_2 &= 0.11, \\ f_3 &= 0.02, \\ f_4 &= 0.11, \\ f_5 &= 0.38. \end{aligned}$$

These may be compared with the probabilities of occurrence when  $\beta=0$

$$\begin{aligned} f_1 &= 0.0625, \\ f_2 &= 0.25, \\ f_3 &= 0.375, \\ f_4 &= 0.25, \\ f_5 &= 0.0625. \end{aligned}$$

<sup>17</sup> D. A. Kleinman and W. G. Spitzer, Phys. Rev. **118**, 110 (1960).

<sup>18</sup> M. V. Hobden and J. P. Russell, Phys. Letters **13**, 39 (1964).

<sup>19</sup> S. S. Jaswal, Phys. Rev. **137**, 302 (1965).

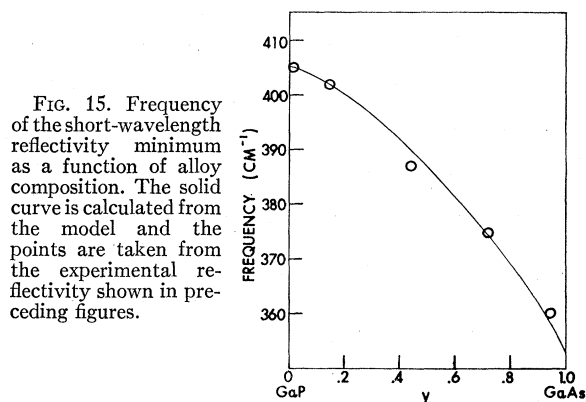


FIG. 15. Frequency of the short-wavelength reflectivity minimum as a function of alloy composition. The solid curve is calculated from the model and the points are taken from the experimental reflectivity shown in preceding figures.

Our original observation, based on the reflectivity data, that there appears to be a high degree of independence of the Ga-As and Ga-P interactions led us to a model which required clustering of like-negative ions to give a reasonable fit to the experimental data. Whereas the theoretical fits are by no means exact they show the significant features of the spectra and we consider them satisfactory in view of the simple, harmonic force model used.

The shift of the GaP band with  $y$  can serve as a measure of the arsenic concentration in a mixed crystal.<sup>20</sup> The spectral feature easiest to observe is the high-frequency reflectivity minimum which occurs very close to the highest frequency longitudinal optic phonon mode. Figure 15 shows the frequency of the reflectivity minimum calculated from the model; and some experimental points where the reflectivity minimum is measured and the concentration is determined by the x-ray method. For an insulating mixed crystal of  $\text{GaAs}_y\text{P}_{1-y}$ , a measurement of the frequency of the reflectivity minimum can be used together with the information in Fig. 15 to determine the composition  $y$ . For crystals with  $10^{17}$  or more carriers present the longitudinal optic phonon and the reflectivity minimum are shifted to higher frequencies. A determination of the composition can still be made, however, using the strongest transverse phonon frequency in the GaP band. This frequency is practically unaffected by the presence of carriers but it is somewhat harder to determine experimentally without curve fitting.

One might object that with the high value of  $\beta(0.75)$  used in most cases, our second assumption, that each negative ion has the same average set of second neighbors, is not valid. For example with  $\beta=0.75$  and  $y=0.5$  the 12 second neighbors of a negative ion are 6 As and 6 P ions divided as follows:

$$\begin{aligned} &4.56 \text{ As}(1) \quad \quad \quad \text{ions,} \\ &1.0 \text{ As}(2) \quad \text{and} \quad 0.33 \text{ P}(2) \text{ ions,} \\ &0.12 \text{ As}(3) \quad \text{and} \quad 0.12 \text{ P}(3) \text{ ions,} \\ &0.33 \text{ As}(4) \quad \text{and} \quad 1.0 \text{ P}(4) \text{ ions,} \\ & \quad \quad \quad \quad \quad \quad \quad 4.56 \text{ P}(5) \text{ ions.} \end{aligned}$$

<sup>20</sup> T. S. Benedict, J. Electrochem. Soc. **110**, 264c (1963).

The unphysical fractional ions arise from our probability approach. It would seem that with the high values of  $\beta$  used in the fits, regions of pure GaAs and pure GaP must exist over several atomic diameters. Such regions are in violation of our assumption that any anion sees the same average distribution of anions as second neighbors. An improved approach would be to consider as basic units a negative ion with its 4 nearest and 12 next-nearest neighbors. Applying similar probability arguments to these large basic units we would have 31 modes and a  $31 \times 31$  dynamical matrix. The fitting of 31 modes is obviously not justified by the reflectivity data. Thus the determination of clustering beyond nearest neighbors is probably difficult though the extension of the model is straightforward conceptually.

A physical reason for the appearance of small clusters in vapor grown crystals may be the transport of As and P as  $As_4$ ,  $As_2$ ,  $P_4$ , and  $P_2$  molecules in the vapor phase.<sup>21</sup> The molecules in the vapor must, of course, break up to form the bonds with the Ga ions. Little is known of this transitional stage between vapor and solid, and it is possible that our suggestion that the constituent ions remain close together, is incorrect. Yet, whatever the mechanism of formation, our results establish a strong case for the actual existence of the clusters.

The confirmation of the existence of nonlocal and local portions of the effective ionic charges of GaP and GaAs is a second important result of our work. The smallness of the local charge of GaP as compared to the one for GaAs is somewhat surprising but is in line with the low ionicity of GaP.

#### ACKNOWLEDGMENTS

The authors gratefully acknowledge valuable discussions with Professor H. Hartmann and Dr. D. E.

McCumber. In addition, the authors are indebted to Dr. D. W. Taylor who pointed out the local-mode enhancement in an ionic lattice and carried out a calculation for the ionic case.

#### APPENDIX: NORMAL-MODE STRENGTHS AND FREQUENCIES

To proceed with the solution of Eqs. (13), (14), and (15) to obtain the infrared active modes, we restrict the wave vectors of all waves to be zero and substitute  $\exp(-i\omega t)$  for the time dependence of all variables. The driving term in the equations of motion consists of two parts for transverse waves.  $E$  (the macroscopic field) which acts on the total ion charge and  $4\pi P_{100}/3$  which acts only on the local part of the ion charge. A typical driving term [Eq. (13)] is therefore expanded as

$$f_1 e_g E_{\text{eff}} = f_1 e_{g1} E + f_1 e_{g1} \left\{ E + \frac{4\pi N}{3} \sum_{j=1}^5 [f_j e_{g1}(j) w_g(j) + f_j x(j) e_{a1} w_a(j) + f_j (1-x(j)) e_{p1} w_p(j)] \right\} \quad (\text{A1})$$

where we have eliminated  $P_{100}$  using Eq. (20). Because of the neutrality requirement, the Ga-ion charge in the  $i$ th unit is the linear combination of As ion and P ion charge that makes the unit neutral. We have therefore

$$\begin{aligned} e_g(i) &= e_{g1}(i) + e_{gnl}(i), \\ e_{g1}(i) &= +x(i)e_{a1} + (1-x(i))e_{p1}, \\ e_{gnl}(i) &= +x(i)e_{a1} + (1-x(i))e_{pnl}, \end{aligned} \quad (\text{A2})$$

as used earlier in Eqs. (13) and (17).

We now write out the first equation of motion to show the types of terms which appear. For the restoring force on a Ga ion in unit 1 we have

$$\begin{aligned} -\omega^2 f_1 m_g w_g(1) &= -f_1(x(1)k_1(1) + [1-x(1)]k_2(1) + yk_7 + (1-y)k_8 + k_6)w_g(1) \\ &+ f_1 \left[ \sum_{j=1}^5 (k_6 f_j w_g(j) + k_7 x(j) f_j w_a(j) + k_8 [1-x(j)] f_j w_p(j)) \right] \\ &+ \frac{4\pi}{3} N [f_1 e_{g1}(1) \sum_{j=1}^5 (f_j e_{g1}(j) w_g(j) - f_j x(j) e_{a1} w_a(j) - f_j [1-x(j)] e_{p1} w_p(j))] + f_1 e_g(1) E. \end{aligned} \quad (\text{A3})$$

The first two terms on the right side of Eq. (A3) are the restoring forces from short-range interactions; the third term contains the additional restoring force arising from dipolar effects. Note that this term contains local charges only. The last term shows that the macroscopic field drives the total charge.

It is convenient now to relabel the ion displacements as  $w(j)$  with  $j=1$  to 13. The first five  $w(j)$  give the Ga-ion displacements in units 1 to 5, the next four give the As ion displacements in units 1 to 4 (there is no As in unit 5), and so on. Using this 13-component displacement vector the equations of motion are compactly written as

$$-\omega^2 \mathbf{M} \mathbf{w} = -\mathbf{K} \mathbf{w} + (4\pi N/3) \mathbf{C} \mathbf{w} + \mathbf{e} E, \quad (\text{A4})$$

<sup>21</sup> J. N. Friend, *Textbook of Inorganic Chemistry* (Griffin, London, 1934), Vol. 6, pts. 2 and 4.

where we have defined the (diagonal) mass matrix  $\mathbf{M}$  ( $M_{11}=f_1m_g$ ,  $M_{22}=f_2m_g$ , etc.), and the charge vector  $\mathbf{e}$  [ $e_1=f_1e_g(1)$ ,  $e_2=f_2e_g(2)$ , etc.].  $\mathbf{K}$  and  $(4\pi N/3)\mathbf{C}$  are the short-range and dipolar force constants. We thus have the standard harmonic lattice vibration problem with the exception that the masses, forces, and charges are not fixed. These quantities all depend on concentration  $y$  and clustering  $\beta$  through the recurring probability factors  $f_i$ ,  $f_i x(i)$  and  $f_i(1-x(i))$ .

To solve Eq. (A4) we combine the short-range and dipolar force matrices to form the dynamical matrix  $\mathbf{D}$ .

$$\mathbf{D} = \mathbf{K} - (4\pi N/3)\mathbf{C}. \quad (\text{A5})$$

The mass is eliminated from Eq. (A4) by left multiplication by  $\mathbf{M}^{-1/2}$  and insertion of the identity matrix  $\mathbf{I} = \mathbf{M}^{-1/2}\mathbf{M}^{1/2}$ . Carrying out these steps we obtain

$$-\omega^2\mathbf{M}^{1/2}\mathbf{w} = -\mathbf{M}^{-1/2}\mathbf{D}\mathbf{M}^{-1/2}\mathbf{M}^{1/2}\mathbf{w} + \mathbf{M}^{-1/2}\mathbf{e}E.$$

Thus with new coordinates  $\mathbf{u} = \mathbf{M}^{1/2}\mathbf{w}$  and a redefined force matrix and charge vector we have the standard eigenvalue problem

$$-\omega^2\mathbf{u} = -\mathbf{D}'\mathbf{u} + \mathbf{e}'E. \quad (\text{A6})$$

Since  $\mathbf{D}'$  is real and symmetric it can be diagonalized to yield the 13 eigenvalues  $\omega_j^2$  by the similarity transformation  $\mathbf{S}$ .

Transforming to the diagonal representation we have

$$-\omega^2\mathbf{v} = - \begin{bmatrix} \omega_1^2 & & & 0 \\ & \omega_2^2 & & \\ & & \dots & \\ 0 & & & \omega_{13}^2 \end{bmatrix} \mathbf{v} + \mathbf{e}''E, \quad (\text{A7})$$

where

$$\begin{aligned} \mathbf{v} &= \mathbf{S}^{-1}\mathbf{u} = \mathbf{S}^{-1}\mathbf{M}^{1/2}\mathbf{w}, \\ \mathbf{e}'' &= \mathbf{S}^{-1}\mathbf{e}' = \mathbf{S}^{-1}\mathbf{M}^{-1/2}\mathbf{e}. \end{aligned}$$

The solutions of Eq. (A7) are simply

$$\begin{aligned} \mathbf{v}_1 &= (e_1'', 0, \dots, 0)E/(\omega_1^2 - \omega^2), \\ &\vdots \\ \mathbf{v}_{13} &= (0, 0, \dots, e_{13}'')E/(\omega_{13}^2 - \omega^2). \end{aligned}$$

The diagonalization has been carried out with a computer to yield the eigenvalues  $\omega_j$ . These are the required mode frequencies. To obtain the mode strengths we transform the polarization equation to the diagonal representation and evaluate the dielectric constant. In our matrix notation the polarization is

$$P = N\mathbf{e} \cdot \mathbf{w} + N\alpha E. \quad (\text{A8})$$

Transforming to the diagonal representation we obtain

$$\begin{aligned} P &= N\mathbf{e}'' \cdot \mathbf{v} + N\alpha E \\ &= \frac{N(e_1'')^2 E}{\omega_1^2 - \omega^2} + \dots + \frac{N(e_{13}'')^2 E}{\omega_{13}^2 - \omega^2} + N\alpha E. \end{aligned} \quad (\text{A9})$$

The dielectric constant is given by

$$\begin{aligned} \epsilon &= 1 + 4\pi P/E \\ &= \frac{4\pi N(e_1'')^2}{\omega_1^2 - \omega^2} + \frac{4\pi N(e_2'')^2}{\omega_2^2 - \omega^2} + \dots + \frac{4\pi N(e_{13}'')^2}{\omega_{13}^2 - \omega^2} \\ &\quad + (1 + 4\pi N\alpha). \end{aligned} \quad (\text{A10})$$

The diagonalization has thus separated the dielectric constant  $\epsilon$  into a sum of independent modes with the frequencies  $\omega_j$  and strengths  $4\pi\rho_j = 4\pi N(e_j'')^2/\omega_j^2$  using the usual notation. In addition to the oscillator modes, there appears the frequency-independent term  $1 + 4\pi N\alpha$  which we call  $\epsilon_\infty$ . Since our model does not include damping, we enter a dimensionless phenomenological damping constant  $\Gamma_j$  for each mode so that we have

$$\epsilon(\omega, y, \beta) = \epsilon_\infty + \sum_j \frac{4\pi\rho_j\omega_j^2}{\omega_j^2 - \omega^2 - i\omega\Gamma_j\omega_j}. \quad (\text{A11})$$

The  $y$  and  $\beta$  parameters are shown explicitly since the mode frequencies and strengths depend on them. Values for  $\omega_j$  and  $4\pi\rho_j$  resulting from diagonalizing the system are given in the figures for the various  $\text{GaAs}_y\text{P}_{1-y}$  alloys studied.